A Numerical Study of Dispersion and Local Exhaust Capture of Aerosols Generated from a Variety of Sources and Airflow Conditions

Madsen, U.; Fontaine, J. R.; Nielsen, Peter Vilhelm; Aubertin, G.; Breum, N. O.

Published in:
American Industrial Hygiene Association Journal

Publication date:
1996

Document Version
Early version, also known as pre-print

AMERICAN INDUSTRIAL HYGIENE ASSOCIATION JOURNAL 57:134–141 (1996)

A Numerical Study of Dispersion and Local Exhaust Capture of Aerosols Generated from a Variety of Sources and Airflow Conditions

AUTHORS
Ulla Madsen[a]
Jean Raymond Fontaine[b]
Peter V. Nielsen[c]
Gérard Aubertin[b]
Niels O. Breum[a]

[a]National Institute of Occupational Health, Lersoe Parkalle 105, DK-2100 Copenhagen, Denmark; [b]INRS, Avenue de Bourgogne, B.P. 27, F-54501 Vandoeuvre Cedex, France; [c]Aalborg University, Sohngaardsholmsvej 57, DK-9000 Aalborg, Denmark

Focus is put on aerosol source parameters and their influence on aerosol dispersion and capture by a local exhaust. The studied parameters were particle diameter, density, and initial velocity. Included in the study was the influence of obstacles and airflow patterns. Direct capture efficiency of an exhaust above the contaminant source was used to compare the influence of the studied parameters. The study was based on a numerical model that computes the particle trajectories, taking inertia, drag forces, gravity, and turbulence into account. The relevance of particle relaxation time, aerodynamic diameter, and stopping distance is discussed. It is concluded that local exhaust capture of passively emitted particles can be described by particle relaxation time and the vertical air velocity at the emission point. The influence on direct capture efficiency from particle initial velocity is limited compared to imposed airflow patterns as jets and cross drafts. A table underneath the contaminant source may improve capture efficiency. The numerical model proved to be a useful tool to handle the complexity of contaminant sources in the industrial environment.

Keywords: aerosol source parameters, aerosol dispersion, local exhaust capture, numerical model

In most numerical and many laboratory studies of contaminant dispersion and local exhaust capture, the source is regarded as a passive point source, located free of obstacles. Real contaminant sources are much more complex and cannot be simulated by a passive point source. In a pilot study Madsen and Tveit[1] studied capture efficiency of a local exhaust at a can filling machine common in the paint industry. The configuration used is shown in Figure 1. Detail A pictures exhaust of organic solvents evaporating from a can. For comparison, Detail B pictures exhaust of a passive contaminant emitted from a point source of simple geometry. Data obtained on local exhaust capture efficiency are included in the figure. As can be observed from the figure, the simple point source (B) is insufficient for simulating the complex source (A). This is even more so for sources emitting particulate contaminants. For such sources particle diameter may have a substantial influence on local exhaust capture efficiency.[2] However, it is recognized that in most studies it is impossible to include all details of the contaminant source and the room under investigation.

The purpose of the present study was to develop, using a numerical model, a method for characterization of the influence on contaminant dispersion and local exhaust capture of a variety of sources and conditions. Particles were selected for contaminants, and the parameters under investigation included basic particle characteristics (diameter, density, and initial velocity) and common airflows (jet of air, cross draft, and altered airflows due to obstacles). The study was limited to point sources and steady, isothermal conditions.

To compare the influence of different contaminant parameters, direct capture efficiency of a local exhaust next to the contaminant source was chosen as an indicator. This indicator is a well-established tool among occupational hygienists for evaluating the performance of local exhaust systems.[3] Models on which the study is based are summarized first. It is emphasized that no attempt is made to develop a general equation

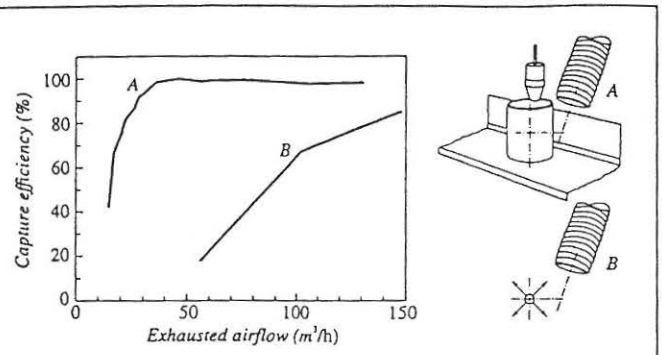

FIGURE 1. Capture efficiency versus exhausted airflow of a local exhaust at a can filling machine (A) and a simple point source (B). The distances are identical from the exhaust openings to center of the can and the point source, respectively. Tracer gas is used as a simulated contaminant for measuring local exhaust capture efficiency. Madsen and Tveit.[1]

for estimation of local exhaust capture efficiency as a function of a list of parameters, nor to validate the numerical model by experimental data.

Local Exhaust Capture Efficiency

Consider a local exhaust opening at a source of constant emission rate, S, there being only one source in the room. At steady state the capture rate of the exhaust is S_{le}. Then the total capture efficiency is

$$\eta_{le}^{tot} = \frac{S_{le}}{S} \quad (1)$$

Consider a room with a single exhaust opening. Due to mass-balance, contaminants emitted in the room must leave by the exhaust (no sink effects). At steady-state any opening would have a 100% total capture efficiency, even though the opening may be located far away from the contaminant source. Consequently, the concept of total capture efficiency may not be considered a useful parameter in general for characterizing the performance of a local exhaust system. To arrive at a more useful parameter Jansson[4] suggested that S_{le} should include only contaminants being directly captured, but no consistent definition of the term "directly" was given. For this study the term "directly" was defined from an imaginary control box containing the source and the exhaust opening (Figure 2). By definition, contaminants kept within the control box were considered to be captured directly. Let $S_{s,le}$ denote the rate of contaminants being captured directly. Then direct capture efficiency is defined as

$$\eta_{le}^{d} = \frac{S_{s,le}}{S} \quad (2)$$

Emission rate S is considered to be known, but a consistent estimate of $S_{s,le}$ requires detailed recording of trajectories of all fluid elements of contaminant.

Direct capture efficiency depends on size and location of the imaginary control box in relation to the contaminant source and the exhaust opening.[5] However, in this study the control box location was kept constant.

Numerical Model

The dispersion of particles in turbulent flows can be obtained by a Eulerian or Lagrangian method.[6] In the Eulerian method, both the fluid and the particulate phase are regarded as continuous media, whereas in the Lagrangian method, the particles are treated individually through solving the particle motion equation. In this study the Lagrangian method was used for two reasons: (1) It is the only method to study the effect of various particle characteristics, and (2) knowledge of the particle trajectories is needed to obtain the direct capture efficiency of a local exhaust system. The model is described in detail by Lu et al.[6] and will only briefly be presented here. The model has been tested with experimental data and a good agreement was obtained,[7] but it is emphasized that validation of the model for the specific configuration has not been performed.

The motion of a spherical and rigid particle in a fluid flow is governed by the following simplified equations, where inertia equals drag and gravity forces:[6]

$$\rho_p \frac{d\vec{V}}{dt} = -\frac{3}{4d_p}\rho_f C_D(\vec{V} - \vec{U})|\vec{V} - \vec{U}| + (\rho_p - \rho_f)\vec{g} \quad (3)$$

$$\frac{d\vec{X}}{dt} = \vec{V} \quad (4)$$

where $\vec{V}$ and $\vec{U}$: instantaneous particle and fluid velocity, respectively
$\vec{X}$: particle position
ρ_p and ρ_f: particle and fluid density, respectively
d_p: particle diameter
$\vec{g}$: acceleration due to gravity
$C_D = 24/Re_p(1 + 0.15(Re_p)^{0.687})$ is the drag coefficient
$Re_p = |\vec{V} - \vec{U}|d_p/\nu_f$ is the particle Reynolds number
ν_f: kinematic viscosity

A typical example of the motion of particles in front of an exhaust opening is illustrated in Figure 3. Detail A is the airflow pattern; note the effect of the cross draft. Detail B is the flow pattern of particles emitted at point S with an initial velocity in the same direction as the cross draft. The drag force decelerates the particles, while the gravity force accelerates them downward. However, due to turbulence some of the particles are exhausted by the local exhaust.

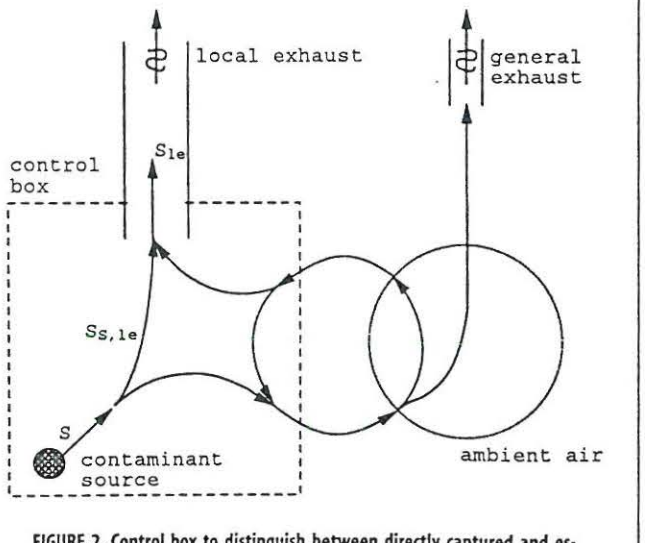

FIGURE 2. Control box to distinguish between directly captured and escaped contaminants. The circle to the right represents room air excluding the control box.

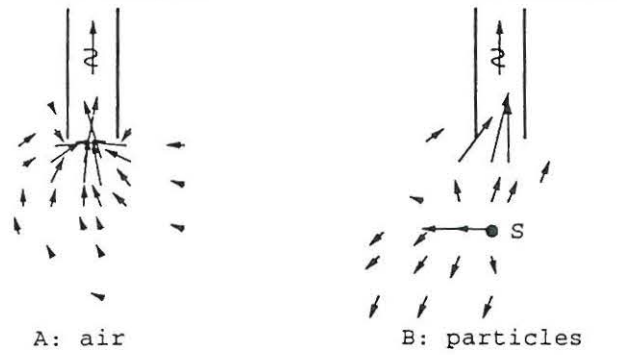

FIGURE 3. Flow pattern of air (A) and particles (B) in front of an exhaust opening at a location with a slight cross draft (redrawn from calculated data). 60 μm particles of unit density are emitted with an initial velocity.

It was assumed that the particle mass-loading is low so that the presence of particles does not modify the fluid motion, nor was interaction between particles taken into account. As this study was limited to particle diameters greater than 1 μm, the Cunningham slip factor was not included in the model. It was further assumed that particle density was much greater than air density. The bulk properties of the particulate phase were obtained by averaging trajectories over a large number of particles, in this study 5000. The particle trajectories were obtained by solving Equations 3 and 4 for successively small time steps Δt (0.002 sec), assuming constant U within each time step. Choice of number of particles and time step was made as a compromise between accuracy and computation time. As directly captured particles were the only ones of interest, computation time was diminished by computing only the trajectories until the particles passed the imaginary control box. Otherwise each particle was followed until it was exhausted by the local exhaust or hit the outer duct wall. A sensitivity analysis for time steps ranging from 0.001 to 0.01 seconds and particle numbers ranging from 5000 to 20,000 did not indicate a substantial influence on the obtained results.

To solve Equation 3 the instantaneous velocity of the fluid, $\tilde{U}$, is required at the location of the particle. The mean velocity is readily obtained from the turbulent fluid flow field computed by the technique of computational fluid dynamics (CFD). The fluctuating velocity of the fluid is modeled from a random process and knowledge of the turbulent kinetic energy, obtained from the CFD-computation. For this study Lagrangian autocorrelation and Eulerian spatial correlation functions presented by Lu et al.[6] were used to relate the fluctuating velocities of the fluid at the successive location points of the particle. The functions include both the time and space effects of the turbulent field.

The mean velocity field and turbulent kinetic energy were computed by the validated CFD-code EOL[8] under isothermal and steady conditions. The two-equation $k-\varepsilon$ turbulence model and the wall functions introduced by Launder and Spalding[9] were used. A relatively fine grid (31 × 21 × 27) was used for all tests, and no grid refinement studies have been made. When $\tilde{X}$ was not at the computation grid points, the mean quantities were obtained from linear interpolation of values at the eight nearest points. If the particle was between grid points and a boundary, the mean quantities were obtained using the wall functions. The particles deposited when they reached a surface.

Direct capture efficiency, η^{d}_{lc}, of the local exhaust was computed by following each particle trajectory and determining if the particle escaped the control box.

Relaxation time, aerodynamic diameter, and stopping distance are useful parameters for characterizing the motion of a particle in a fluid. By introducing the particle relaxation time, τ_p, Equation 3 can be rewritten as

$$\frac{d\tilde{V}}{dt} = -\frac{1}{\tau_p}(\tilde{V} - \tilde{U}) + \frac{\rho_p - \rho_f}{\rho_p}\tilde{g} \qquad (5)$$

where τ_p is given as

$$\tau_p = \frac{d_p^2 \rho_p}{18\mu} \frac{24}{C_D Re_p} \qquad (6)$$

and μ is fluid dynamic viscosity.

In the Stokes regime, that is, for small differences between particle and fluid velocities, Equation 6 reduces to

$$\tau_p = \frac{d_p^2 \rho_p}{18\mu} \qquad (7)$$

There exists a critical relaxation time, $\tau_{p,cr}$, where drag forces become equal to gravity force. Let direction of the gravitational force be denoted −y. Then $\tau_{p,cr}$ is obtained by solving Equation 5 for the y-direction, setting $dV_y/dt = 0$ and $V_y = 0$:

$$\tau_{p,cr} = \frac{U_y}{g\dfrac{\rho_p - \rho_f}{\rho_p}} \approx \frac{U_y}{g} \qquad (8)$$

where U_y is the fluid velocity in the y-direction at the emission point.

The aerodynamic diameter, d_{ae}, of a particle is defined as the diameter of a spherical particle of unit density (ρ_0 = 1000 kg/m³) having a settling velocity identical to the particle under consideration. The diameter is related to particle relaxation time by

$$d_{ae}^2 = \frac{\tau_p 18\mu}{\rho_0} \simeq d_p^2 \frac{\rho_p}{\rho_0} \qquad (9)$$

Note that the approximation is valid only in the Stokes regime.

Particle stopping distance, l, is defined as

$$l = \tau_p |\tilde{V} - \tilde{U}| \qquad (10)$$

and is the distance a particle travels in quiescent air before it comes to rest. Note that τ_p should be calculated from Equation 6 using the actual particle Reynolds number. τ_p increases with decreasing particle velocity and approaches τ_p calculated from Equation 7 as the particle reaches air velocity.

Test Room Configuration

The configuration of the room being modeled is shown in Figure 4. The air supply rate was 427 m³/hr for all tests (air exchange rate of 10 hr^{-1}). The exhausted flow rates were 327 m³/hr at the general exhaust, and 100 m³/hr at the local exhaust. The contaminant was released in the center line of the local exhaust, 0.20 m below the exhaust opening. To compute direct capture efficiency, the imaginary control box was kept at the position shown in Figure 4 with the dimensions 0.60 × 0.60 × 0.60 m.

Contaminant and Airflow Parameters Under Testing

It is well known that particle diameter, density, and initial velocity are important for the dispersion and local exhaust capture

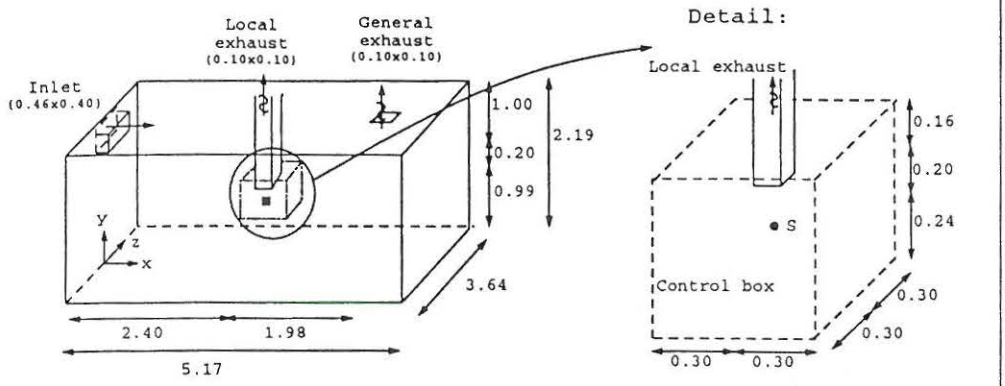

FIGURE 4. Configuration of the test chamber including the imaginary control box. Dimensions are given in meters.

of aerosols.[10] Other parameters may be of importance, including geometry and location of the source and airflow patterns in the area of the source. In this study particle diameter, density, and initial velocity were selected for a detailed analysis. Three types of patterns—i.e., jet of air, cross draft, and altered airflow due to obstacles—were also subjected to analysis. All results presented in this article were obtained from numerical computations.

Particle Characteristics

Particle diameter was studied in the range from 1 μm to 100 μm. The chosen densities corresponded to the following materials: wood (600 kg/m^3), sand (1600 kg/m^3), concrete (2300 kg/m^3), and steel (7200 kg/m^3). Unit density (1000 kg/m^3) was included as a reference. The corresponding particle relaxation times ranged from 10^{-6} to 10^{-1} sec. For testing of capture efficiency versus particle initial velocity, velocity of a jet and cross draft, a limited number of particle sizes was used (1, 10, 30, and 60 μm particles of unit density). For selected cases with high particle Reynolds numbers, an investigation was carried out comparing the local exhaust capture of different particles with the same aerodynamic diameter. Results were obtained for 11 μm particles with a density of 7200 kg/m^3 equivalent to an aerodynamic diameter of 30 μm.

In the industrial environment, processes like grinding may emit particles with a high initial velocity, e.g. 50 m/sec.[11] Particle initial velocity was studied in the range from 2 to 50 m/sec, equivalent to particle stopping distances ranging from 10^{-3} to 10^{-1} m. The particles were emitted perpendicular to the source-duct axis and towards the exhaust opening, respectively.

Airflow Patterns

Air jets at emission areas of contaminants may occur in several work processes, including paint spraying by compressed air and shielded gas welding. Air velocities ranging from 0.1 to 1.0 m/sec were studied. The jet operated over an area of 0.025 × 0.025 m and was directed perpendicular to the source-duct axis. Particle initial velocity was equal to velocity of the jet.

Cross draft is another type of air movement that may deteriorate the capture efficiency of a local exhaust. Several authors have studied the influence of cross draft on capture efficiency for passive point sources.[3,12,13] In this study the influence of a uniform cross draft on local exhaust capture of particles was investigated for cross draft velocities ranging from 0.10 to 0.225 m/sec, which are common in industrial premises. The cross draft was imposed on the right side of the imaginary control box (x = 2.70 m), shown in Figure 4.

Introduction of obstacles will more or less alter the airflow in a room compared with an empty room. The influence of altered airflows caused by an obstacle close to the contaminant source was investigated by introducing a table 0.09 m below the source. The table was 1.25 × 0.80 m and centered at the exhaust duct axis. This configuration was chosen as being representative of situations where the contaminating process takes place above a table.

RESULTS

The reasonableness of the velocity fields was evaluated from vector plots. For briefness vector plots are not included here. The normalized sum of the absolute residuals for the equation of continuity was less than 2% for all tests.

Particle Characteristics

In Figure 5 direct capture efficiency is given versus particle relaxation time and aerodynamic diameter, respectively. The particles were passively emitted into a weak cross draft (0.05 m/sec). τ_p was calculated from Equation 7. It is stressed that the results were obtained from combinations of particle diameter and density. The mean fluid velocity at the emission point in the y-direction

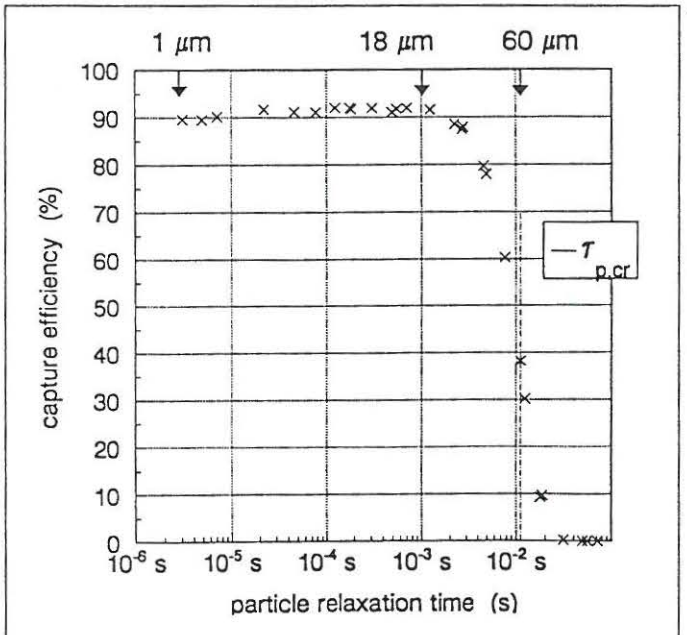

FIGURE 5. Direct capture efficiency versus particle relaxation time and aerodynamic diameter, respectively

was 0.11 m/sec, giving a critical relaxation time (Equation 8) of 0.011 sec.

Direct capture efficiency versus particle initial velocity is given in Figure 6 for particles emitted perpendicular to the source-duct axis and towards the exhaust opening, respectively. In Figure 7 direct capture efficiency normalized with the efficiency for no initial velocity is given versus particle stopping distance for three particle relaxation times. τ_p was computed from Equation 6 based on the particle initial velocity. Included in the figure are examples of τ_p computed from Equation 7 and direct capture efficiency obtained by displaced emission point equivalent to the given stopping distance.

Airflow Patterns

Direct capture efficiency versus air velocity of a jet is given in Figure 8. The air velocity of the jet was the velocity at the outlet of the nozzle shown on Figure 8 to the right. Penetration depth of a jet of air was defined as the distance from the inlet to the point where the jet velocity has decreased to ambient air velocity. The jet of air under investigation had a penetration depth of approximately 0.1 m (0.10 m/sec inlet velocity), 0.3 m (0.50 m/sec inlet velocity), and 0.7 m (1.00 m/sec inlet velocity). Observing Figures 6 and 8 together, it is observed that capture efficiency for low jet velocities was almost 100%, and was only 90% for particles emitted at a low velocity. These two situations could be considered almost identical, and the observed inconsistency is commented on in the discussion.

Direct capture efficiency versus cross draft velocity is given in Figure 9. The cross draft velocity was the velocity imposed 0.30 m from the contaminant source as indicated to the right on Figure 9. It is noted that the vertical air velocity at the emission point was reduced from 0.11 m/sec to 0.08 m/sec. A probable explanation is that the local exhaust was supplied with air from the cross draft, and consequently less air was exhausted from the remaining surroundings. The cross draft caused by the general ventilation of the chamber was approximately 0.05 m/sec. Observing Figures 6 and 9 together, it is found that capture efficiency for 1, 10, and 30 µm particles emitted into a weak cross draft (0.10 m/sec) was almost 100% and was only 90% with no cross draft. This finding is further commented on in the discussion.

The altered airflow caused by a table below the contaminant source increased direct capture efficiency from 89.5% (no table) to 97.5% (with table). The contaminant was 1 µm particles of unit density.

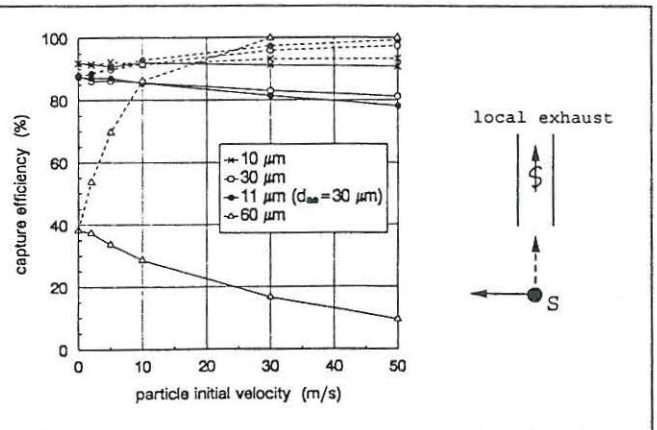

FIGURE 6. Direct capture efficiency versus particle initial velocity, for particles emitted horizontally (solid lines) and vertically (dashed lines)

DISCUSSION

Particle Characteristics

The influence of particle relaxation time on direct capture efficiency is shown in Figure 5. It appears that direct capture efficiency was nearly independent of τ_p below a limit of 0.001 sec (d_{ae} = 18 µm). Above this limit capture efficiency decreases rapidly due to the increasing influence of gravity. For τ_p above 0.03 sec all particles settled to the floor. The critical relaxation time, $\tau_{p,cr}$, is indicated in the figure. As would be expected, $\tau_{p,cr}$ was in the transition region where the local exhaust looses its capture ability. Due to turbulence some particles with a τ_p larger than $\tau_{p,cr}$ were exhausted and vice versa.

Tracer gas techniques have proved to be useful for estimating local exhaust capture efficiency of gaseous contaminants.[3] However, simulating aerosols with tracer gas has not been fully tested. From this study it appears that tracer gas techniques can be used to simulate the capture of particles having an aerodynamic diameter less than 18 µm. Hampl and Shulman[2] measured local exhaust capture efficiency using tracer gas and particles as contaminants. They found that the capture of particles above 3 µm can be simulated by tracer gas only if correction factors are used. This finding is inconsistent with the present study. However, a universal aerodynamic diameter does not exist below which aerosols can be simulated by a tracer gas, but depends on how sensitive the measured parameter (e.g., capture efficiency) is to differences between flow of air and particles, respectively. Particles are unable to follow the air instantaneously due to their inertia in accelerating and decelerating airflows, as well as to changes in airflow direction. This effect has been observed for particles down to 0.5 µm.[14] Other effects such as deposition[15] and turbulence[16] enhance the divergence between flow patterns of air and particles, respectively. Adam et al.[15] measured exchange rates of tracer gas and oil-smoke particles in a ventilated test chamber. They found that exchange rates of particles down to 0.5 µm were higher than the tracer gas exchange rate due to deposition on surfaces. It is stressed that a critical particle size of 18 µm is valid only for this specific test configuration. Other sets of parameters, including distance between the source and exhaust opening, flow rate of exhausted air, and disturbing airflows are expected to result in other critical particle sizes.

From Figure 5 it appears that $\eta_{le}{}^{d}$ slightly increases for τ_p up to 0.001 second. This can be explained by the fact that particle inertia decreases the ability of the particles to follow the fluid fluctuations,[16] and therefore they disperse less about their mean trajectory. It influences direct capture efficiency, as turbulent dispersion and gravity are the only mechanisms by which particles may escape the local exhaust.

Direct capture efficiency versus particle initial velocity is shown in Figure 6. Particle initial velocity had a negative effect on capture efficiency for particles emitted perpendicular to the duct axis, while particles emitted towards the exhaust opening caused an increase in direct capture efficiency. This is to be expected, as air velocity, and consequently capture ability, increases with decreasing distance to the exhaust opening.

As observed in Figure 7, direct capture efficiency normalized with the efficiency, for no initial velocity is more sensitive to stopping distance for the larger particles than the smaller particles: Though the stopping distance is the same, particles with a substantial relaxation time will settle to the floor in the case of horizontal emission, while particles with a low relaxation time will follow the air after they have lost their initial momentum and return into the exhaust. This finding indicates that the capture ability of a

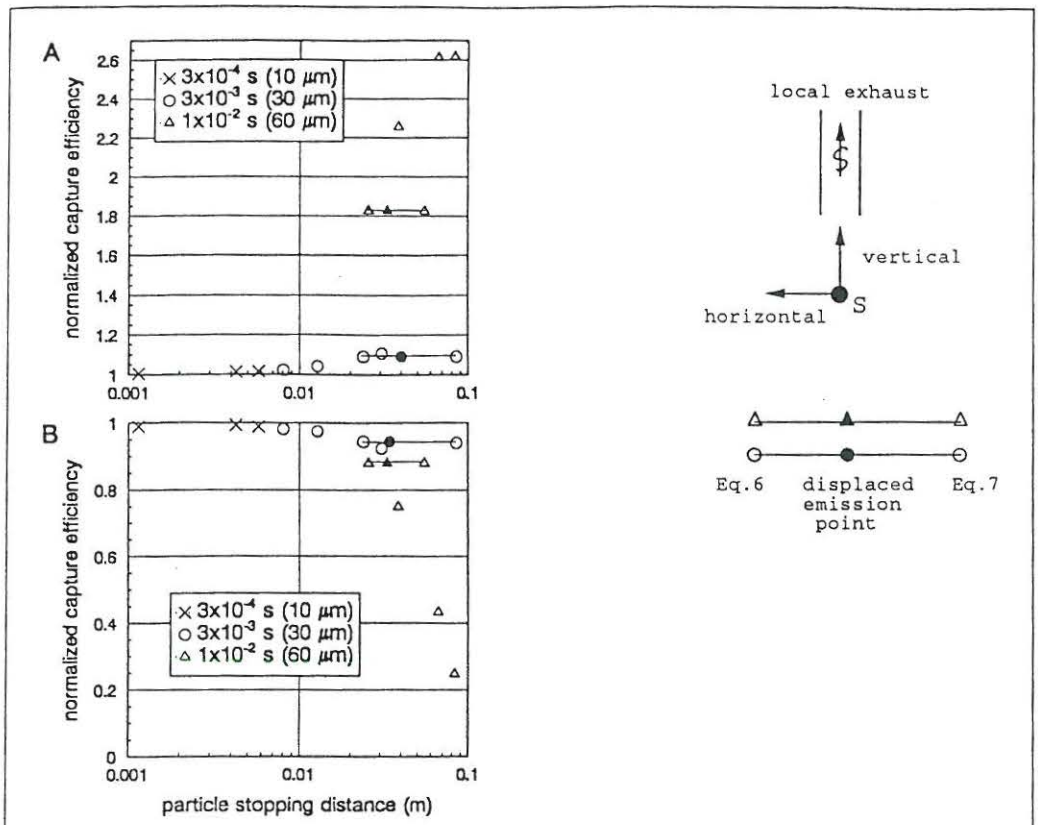

FIGURE 7. Direct capture efficiency normalized with capture efficiency for passively emitted particles versus particle stopping distance. Detail A was obtained for particles emitted vertically, and Detail B was obtained for particles emitted horizontally.

local exhaust cannot be described by particle stopping distance alone.

τ_p calculated from Equation 6 based on particle initial velocity underestimated particle stopping distance, while using Equation 7 overestimated stopping distance. This is confirmed by the results from displaced emission (see Figure 7). It is noted that particle stopping distance is of importance for personal exposure to dust. Hamill et al.[17] studied the exposure to wood dust from rotating woodworking machines. They compared the theoretical particle stopping distance with the distance between the work piece (emission point) and the operator, and found that the larger particles (> 300 μm) were able to reach the operator.

Airflow Patterns

In the case of particles being emitted with an initial velocity, the ambient air is seldom calm. In field studies it is difficult to separate the effect of the dispersion process from particle initial velocity and air movements.[17] However, the numerical model of this study offers this opportunity. Airflows at a contaminant source in the industry may be generated by several conditions, including moving parts of machines, forced ventilation, or buoyancy driven airflow.

In this study the influence of a jet of air at the emission area was investigated for air escaping a nozzle at the particle emission point. Capture efficiency versus air jet velocity is shown in Figure 8 for selected particle diameters. Though the jet was working over a small area (0.6% of the local exhaust area) the influence was substantial. For a jet velocity of 1.0 m/sec the local exhaust had no effect, and for larger particles 0.1 m/sec was sufficient to make them escape the exhaust. Hall et al.[18] studied numerically the effect of a similar jet in a test cabin. As the momentum of the jet was much higher than in the present study, it completely dominated the flow patterns of air and particles. Fletcher and Johnson[19] studied local exhaust capture efficiency for various jet velocities and directions by use of tracer gas. They found that for a jet oriented away from the exhaust, capture efficiency was inversely proportional to the momentum of the jet. For a jet oriented perpendicular to the exhaust duct, the momentum of the jet (equivalent to a jet velocity of 0.13 m/sec in the present study) was too low to influence capture efficiency. Cornu[20] concluded from a chamber study

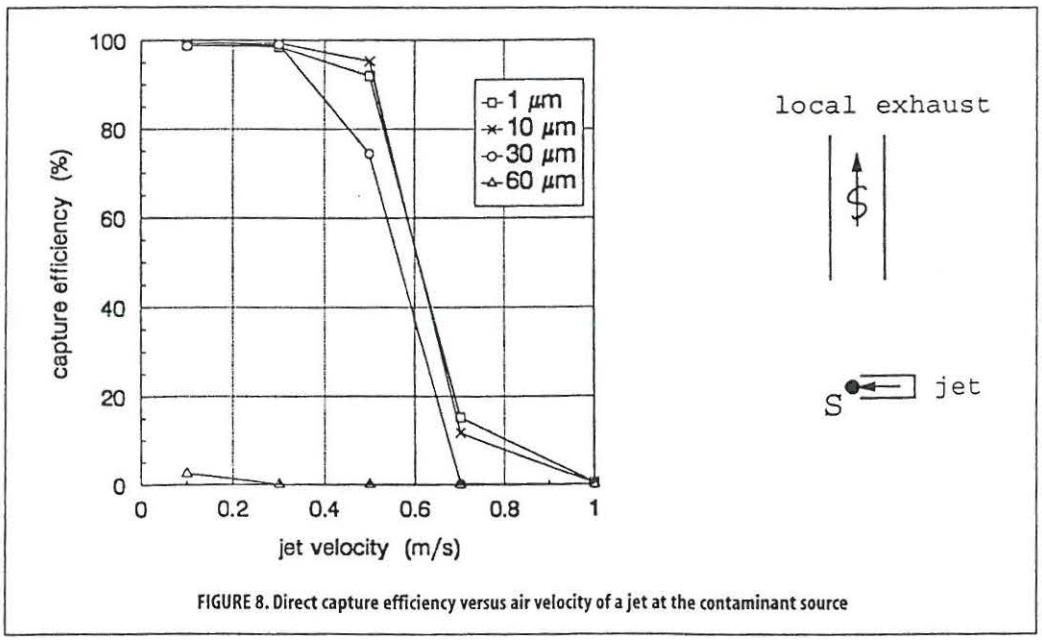

FIGURE 8. Direct capture efficiency versus air velocity of a jet at the contaminant source

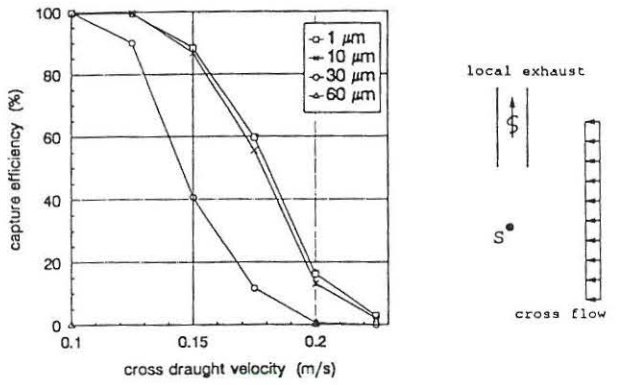

FIGURE 9. Direct capture efficiency versus cross draft velocity

that the flow of shielding gas in gas-metal-arc welding enhanced the spread of generated welding fumes and deteriorated capture efficiency of the local exhaust system under investigation.

As already mentioned, data in Figure 6 seem inconsistent with Figure 8, as capture efficiency for small air jet velocities was almost 100% but only 90% for particles emitted at a low velocity. The results indicate different flow conditions, and this observation is unexpected. Causes for this difference may include altered airflows and an insufficient numerical model. Introduction of small obstacles such as the one used with the air jet (Figure 8, to the right) might alter the airflow, including its turbulent behavior. Though air velocity of the jet is low, the jet itself might influence the general flow pattern as well. The numerical model might be insufficient in several aspects, including the turbulence model and the temporal and spatial resolution. However, a detailed analysis of the numerical model was not the purpose of this article, and further studies are needed to sort out the observed inconsistency.

Direct capture efficiency versus cross draft velocity is given in Figure 9. As can be observed from the figure, a minor increase in cross draft velocity (e.g., from 0.15 to 0.175 m/sec) caused a drop in capture efficiency from 90 to 60% for 1 µm particles. Most aerosols were blown away from the local exhaust at cross draft velocities above 0.20 m/sec. For a fixed cross-draft velocity, Niemelä et al.[3] did an experimental study on capture efficiency versus air velocity at the emission point. They observed a smaller influence of cross draft than in the present study. This inconsistency may be due to differences in test conditions, including flanges and protecting surfaces. The air velocity at the emission point in the present study was reduced to 0.085 m/sec ($\tau_{p,cr}$ = 0.0087 sec) compared with the situation of no cross draft. This made it impossible for the local exhaust to capture the 60 µm particles (τ_p = 0.011 sec). Comparing Figures 6 and 9, it is noted that capture efficiency for 1, 10, and 30 µm particles emitted into a weak cross draft (0.10 m/sec) was almost 100%, and was only 90% with no cross draft. Perhaps this improvement can be explained by reduced turbulence, which is a consequence of the uniformity of the cross draft.

Viewing Figures 6, 8, and 9 together allows a comparison of the influence of particle initial velocity, air velocity of the jet, and cross draft velocity on capture efficiency. As an example, direct capture efficiency was reduced to 80% for 30 µm unit density particles of a high initial velocity (50 m/sec). A moderate jet velocity (0.5 m/sec) and a small cross draft (0.13 m/sec) gave the same reduction in capture efficiency.

Distorted airflow caused by an obstacle may influence the dispersion of contaminants.[18] In this study a table below the contaminant source increased direct capture efficiency from 89.5% to 97.5%. This is due to the fact that the table reduces the area in front of the exhaust opening, as flanges on exhaust openings do. Consistent observations were reported by Madsen and Tveit.[1] They observed that the can filling machine in Figure 1 increased the local exhaust capture efficiency compared to a point source free of obstacles. Garrison et al.[21] demonstrated in a laboratory experiment that the air velocity in front of an exhaust opening near a solid surface is nearly identical to a combination of the exhaust and its mirror image below the surface. However, some obstacles may have a negative effect. Hall et al.[18] reported a case where an obstacle created a recirculating zone in which the particles were entrained.

Particle Aerodynamic Diameter

It is often assumed in industrial hygiene studies that dispersion of aerosols can be described by the particle aerodynamic diameter, neglecting the actual particle diameter and density. From Equations 5 and 6 it appears that this assumption does not hold for important particle Reynolds numbers. In this study the error was tested versus particle initial velocity (Figure 6). Two particles of identical aerodynamic diameter were used. The difference between the capture of the two particles increased with increasing initial velocity; that is, with increasing particle Reynolds number. However, the differences in capture efficiency were below 3%. Cheng et al.[14] pointed out that the aerodynamic diameter is defined in the Stokes region, where the relative velocity is small, and that for larger velocities the actual particle density is important.

CONCLUSION

From this study it is concluded that local exhaust capture of passively emitted particles can be described by particle relaxation time and the vertical air velocity at the emission point. The influence on direct capture efficiency from particle initial velocity is limited compared with imposed airflow patterns. Larger particles emitted towards the exhaust opening are less influenced by disturbing air currents than are smaller ones. The smaller particles are therefore more difficult to capture in such cases. A table underneath a contaminant source may improve capture efficiency.

This study demonstrates that a correct description of geometric and airflow conditions as well as source parameters is crucial for the obtained local exhaust capture efficiency. The numerical results can therefore only be used for cases like those specified, but it has to be emphasized that the numerical model must be validated experimentally for the specific configurations. To handle the complexity of contaminant sources in the industrial environment, the numerical method described in this article has proved to be useful. Once the specific dispersion and capture mechanisms are understood, efficient methods for contaminant elimination can be developed.

NOMENCLATURE

C_D: drag coefficient (-)
Re: Reynolds number (-)
S: flow rate of contaminant (kg/sec)
U: air velocity (m/sec)
V: particle velocity (m/sec)
X: particle position (m)

d: diameter (m)
g: acceleration due to gravitation (m^2/sec)
k: turbulent kinetic energy (J/kg)
l: particle stopping distance (m)
t: time (sec)
x, y, z: Cartesian coordinates (m)
ε: turbulent dissipation rate (J/kg sec)
η: capture efficiency (-)
μ: dynamic viscosity (Pa sec)
ν: kinematic viscosity (m^2/sec)
ρ: density (kg/m^3)
ρ_0: unit density (kg/m^3)
τ: relaxation time (sec)

Sub- and Superscripts

S: contaminant source
ae: aerodynamic
cr: critical
cross: cross draft
d: direct
f: fluid
le: local exhaust
p: particle
tot: total

References

1. **Madsen, U. and D.J. Tveit:** "Dispersion of Contaminants—Investigation of a Can Filling Process in the Paint Industry." M.Sc. thesis, University of Aalborg, Aalborg, Denmark, 1990. [Danish]
2. **Hampl, V. and S. Shulman:** Use of tracer gas techniques for industrial exhaust hood efficiency evaluation—application of sulfur hexafluoride for hood controlling particulate emissions. *Am. Ind. Hyg. Assoc. J. 46*:379–386 (1985).
3. **Niemelä, R., A. Lefevre, J.P. Muller, and G. Aubertin:** Comparison of three tracer gases for determining ventilation effectiveness and capture efficiency. *Ann. Occup. Hyg. 35*:405–417 (1991).
4. **Jansson, A.:** "Local Exhaust Ventilation and Aerosol Behaviour in Industrial Workplace Air." Ph.D.diss., National Institute of Occupational Health, Sweden, 1990.
5. **Madsen, U., N.O. Breum, and P.V. Nielsen:** A numerical and experimental study of local exhaust capture efficiency. *Ann. Occup. Hyg. 37*:593–605 (1993).
6. **Lu, Q.Q., J.R. Fontaine, and G. Aubertin:** Particle motion in two-dimensional confined turbulent flows. *Aerosol Sci. Tech. 17*:169–185 (1992).
7. **Lu, Q.Q., J.R. Fontaine, and G. Aubertin:** A Lagrangian model for solid particles in turbulent flows. *Int. J. Multiphase Flow 19(2)*:347–367 (1993).
8. **Fontaine, J.R., R. Braconnier, R. Rapp, and J.C. Sérieys:** "EOL: A Computational Fluid Dynamics Software Designed to Solve Air Quality Problems." Paper presented at Ventilation '91: 3rd International Symposium on Ventilation for Contaminant Control, Cincinnati, OH. 1991. pp. 449–460.
9. **Launder, B.E. and D.B. Spalding:** The numerical computation of turbulent flows. *Comp. Meth. Appl. Mech. Eng. 3*:269–289 (1974).
10. **Heinsohn, R.J.:** *Industrial Ventilation: Engineering Principles.* New York: John Wiley & Sons, 1991. p. 171.
11. **National Institute for Occupational Safety and Health (NIOSH):** *Ventilation Requirements for Grinding, Buffing, and Polishing Operations*, by E.K. Bastress, J.M. Niedzwecki, and A.E. Nugent, Jr. [(DHEW/NIOSH pub. no. 75–107] Cincinnati, OH:NIOSH, 1974.
12. **Conroy, L.M. and M.J. Ellenbecker:** Capture efficiency of flanged slot hoods under the influence of a uniform cross draft: Model development and validation. *Appl. Ind. Hyg. 4(6)*:135–142 (1989).
13. **Nielsen, P.V., U. Madsen, and D.J. Tveit:** "Experiments on an Exhaust Hood for the Paint Industry." Paper presented at Ventilation '91: 3rd International Symposium on Ventilation for Contaminant Control, Cincinnati, OH, 1991. pp. 197–201.
14. **Cheng, Y.S., B.T. Chen, and H.C. Yeh:** Behaviour of isometric nonspherical aerosol particles in the aerodynamic particle sizer. *J. Aerosol Sci. 21(5)*:701–710 (1990).
15. **Adam, N.M., J.S. Kohal, and S.B. Riffat:** Effect of ventilation rate on deposition of aerosol particles on materials. *Build. Serv. Eng. Res. & Tech.. 15(3)*:185–188 (1994).
16. **Wells, M.R. and D.E. Stock:** The effects of crossing trajectories on the dispersion of particles in a turbulent flow. *J. Fluid Mech. 136*:31–62 (1983).
17. **Hamill, A., J. Ingle, S. Searle, and K. Williams:** Levels of exposure to wood dust. *Ann. Occup. Hyg. 35*:397–403 (1991).
18. **Hall, D.J., M.A. Emmott, and C. Schofield:** The performance of test cabins for assessing particle emissions from machines—a theoretical study using a numerical model. *Ann. Occup. Hyg. 36*:407–424 (1992).
19. **Fletcher, B. and A.E. Johnson:** "The Capture Efficiency of Local Exhaust Ventilation Hoods and the Role of Capture Velocity." Paper presented at Ventilation '85: International Symposium on Ventilation for Contaminant Control, Toronto, Canada, 1985. pp. 369–390.
20. **Cornu, J.C.:** "A Method for Measuring the Capture Efficiency of Fume-Extracting Welding Guns." Paper presented at Ventilation '91: 3rd International Symposium on Ventilation for Contaminant Control, Cincinnati, OH, 1991. pp. 185–189.
21. **Garrison, R.P., C. Park, and Y. Wang:** "Finite Element Modeling for Velocity Characteristics of Local Exhaust Inlets." Paper presented at Ventilation '88: 2nd International Symposium on Ventilation for Contaminant Control, London, U.K., 1988. pp. 15–24.